

# Laser interferometer with wavefront-reversing mirrors

N. G. Basov, I. G. Zubarev, A. B. Mironov, S. I. Mikhailov, and A. Yu. Okulov

*P. N. Lebedev Physics Institute, Academy of Sciences of the USSR, Moscow*

(Submitted 1 April 1980)

*Zh. Eksp. Teor. Fiz.* **79**, 1678–1686 (November 1980)

A theoretical and experimental investigation was made of a Michelson interferometer with wavefront-reversing mirrors based on stimulated Brillouin scattering. It is shown that the period of the interference pattern obtained when the length of one of the interferometer arms is varied represents the frequency shift due to the stimulated scattering; the visibility curve tends to approach the limit 0.25 and represents a combination of the correlation functions for radiations with different path lengths corresponding to single and double transits across the difference between the interferometer arms. The interferometer can be used for any spatial structure of the exciting radiation and it is insensitive to the optical quality of its components.

PACS numbers: 07.60.Ly, 42.78.Dg, 42.60.By

## 1. INTRODUCTION

Reversal of laser radiation wavefront by nonlinear optics methods is attracting considerable attention. This is primarily due to the unique properties of the radiation reflected from wavefront-reversing mirrors, whose field is identical (apart from the phase factor)

with the complex conjugate of the incident-wave field:

$$E_{\text{refl}}(r_{\perp}) = \text{const } E_{\text{inc}}^*(r_{\perp}).$$

The operation of complex conjugacy is equivalent to reversal of the direction of time in the Maxwell equations and the reflected wave traveling in the opposite direction passes consecutively through all the states

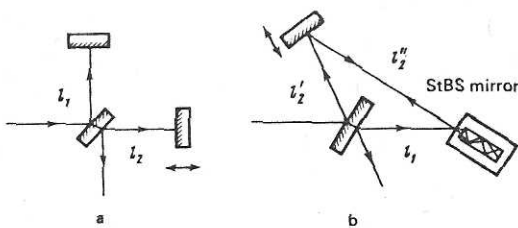


FIG. 1. a) Conventional Michelson interferometer with  $\Delta l = l_2 - l_1$ . b) Interferometer with wavefront-reversing Brillouin mirrors ( $\Delta l = l_2 + l_2' - l_1$ ).

of the incident radiation returning to the initial state. This is why wavefront reversal has been regarded so far mainly as a means for compensating phase distortions suffered by light waves in active elements of laser amplifiers, imperfect optical components, turbulent atmosphere, etc.

We shall show theoretically and experimentally that the use of wavefront-reversing mirrors based on stimulated Brillouin scattering (StBS mirrors) in conventional two-beam interferometers makes it possible to construct systems with new physical properties. By way of example, we shall consider the Michelson (or more exactly, the Twyman-Green) interferometer with plane-parallel light beams in Fig. 1a. In a classical version of this interferometer the waves reflected from the mirrors interfere in a semitransparent mirror and the intensity of the output radiation is given by

$$I \propto [1 + \cos(\pi + \Delta\varphi)].$$

Here,  $\Delta\varphi$  is the phase difference between two light beams acquired in the forward and reverse transits, amounting to  $\Delta\varphi = 2k\Delta l$ , where  $k$  is the wave vector amounting to  $\sim 10^5 \text{ cm}^{-1}$  in the optical range and  $\Delta l$  is the path difference between the interferometer arms.

We can easily see that the direct replacement of the conventional with the wavefront-reversing mirrors in interferometers of this type makes it possible to deal with spatially inhomogeneous instead of plane waves. The profiles of the amplitude of the reflected waves interfering in the semitransparent mirror are now identical and, in view of the relative nature of the field conjugacy on reflection, only the zeroth points may be displaced but the scale of the interference pattern remains the same. The use of two wavefront-reversing StBS mirrors has the effect that even in the case of monochromatic beams the phases of the reflected waves vary in an arbitrary manner from one laser shot to another<sup>1</sup> and, moreover, there may be fluctuations during a laser pulse with a characteristic time  $\tau \sim \Gamma / 2\Delta\nu_{\text{SpBS}}$  (Ref. 2), where  $\Delta\nu_{\text{SpBS}}$  is the width of the spontaneous scattering line and  $\Gamma$  is the gain increment of the scattered wave. This makes it more difficult to observe the interference pattern but also facilitates studies of fluctuations of the phase of the wave scattered in the stimulated Brillouin effect.<sup>3</sup>

Accidental variations of the phases can be eliminated by directing beams produced by division in a semitransparent mirror so they are reflected simultaneous-

ly by the same StBS mirror (Fig. 1b). An interferometer of this kind has fundamentally different characteristics from those discussed above. In fact, as pointed out before, a wavefront-reversing mirror performs an operation on the incident beams which is equivalent to time reversal. Therefore, a beam which has traversed a shorter path before reaching the reversing mirror is reflected with a phase lag amounting to  $k\Delta l$  compared with the second beam. This delay would have been compensated in the reverse path had the frequency of light been unaffected by the reversing mirror and then the reflected beams would have arrived at the semitransparent mirror in phase for any value of  $\Delta l$ . However, since the Brillouin scattering produces a frequency shift of the Stokes component  $\Delta\nu_B$ , the reflected waves reach the semitransparent mirror with some phase difference amounting to  $\Delta\varphi = \Delta k\Delta l = 2\pi\Delta\nu_B\Delta l$  (the frequency shift is measured in reciprocal centimeters).

We can thus see that there is a fundamental difference between systems with independent mirrors and the system discussed above (Figs. 1a and 1b). In the former case a displacement of one of the mirrors by even a fraction of the wavelength alters considerably the difference between the phases of the light beams reaching the transparent mirror ( $\Delta\varphi = 2k\Delta l$ ) because the absolute value of the wave vector is large. In the case of an interferometer with conventional mirrors it is also found that stringent requirements have to be satisfied in respect of the orientation of the mirror when it is displaced (scanned), in respect of its optical quality, and also in respect of the plane-parallel nature of the light beam. In the latter case of reflection of two light beams from the same wavefront-reversing mirror a change in the phase difference at the output of the interferometer with scanning of one of the arms is only due to a change in the frequency of light as a result of reflection. Since the frequency shift in StBS is small ( $10^{-2} - 10^{-1} \text{ cm}^{-1}$ ), the spatial period of the interference pattern amounts to centimeters. Moreover, in the case of reflection with wavefront reversal we can use light beams with any spatial structure and also low-quality beam splitters and mirrors.

Measurements of the interference pattern period can be used to determine the frequency shift in StBS. It should be pointed out that in this analysis it is assumed *a priori* that the laser and scattered radiations are monochromatic. Solid-state lasers with passive Q switching and without additional mode selection emit in practice lines of width  $\Delta\nu_l = 0.1 - 0.1 \text{ cm}^{-1}$ , which is considerably greater than the width of the spontaneous scattering line of practically all the gases ( $\Delta\nu_{\text{SpBS}} \leq 10^{-3} \text{ cm}^{-1}$ ) and some liquids such as  $\text{CS}_2$  ( $\Delta\nu_{\text{SpBS}} \sim 4 \times 10^{-3} \text{ cm}^{-1}$  at the neodymium laser wavelength). Therefore, relative to the active medium, we can regard laser radiation as wide-band:  $\Delta\nu_l \gg \Delta\nu_{\text{SpBS}}$ . In a conventional interferometer when the difference between the paths of the two beams is  $2\Delta l \rightarrow \infty$ , the feasibility of the interference pattern becomes

$$V = \frac{I_{\text{max}} - I_{\text{min}}}{I_{\text{max}} + I_{\text{min}}} \rightarrow 0.$$

The behavior of the visibility curve in the case of an

interferometer with wavefront-reversing StBS mirrors and a laser source emitting a line of width  $\Delta\nu_1 \gg \Delta\nu_{\text{SpBS}}$  will be predicted on the basis of an analysis of the relevant dynamic equations and explicit expressions will be obtained for the temporal structure of the reflected waves.

## 2. STIMULATED SCATTERING OF TWO SPATIALLY INHOMOGENEOUS NONMONOCHROMATIC BEAMS

Wavefront reversal in the case of stimulated scattering of a spatially inhomogeneous nonmonochromatic pump wave has already been considered before.<sup>4-6</sup> For example, it is shown in Ref. 4 that in the case of "factorized" pumping, i.e., when the pump wave obeys the condition

$$\varepsilon_p(t, r) = T(t)P(r), \quad (1)$$

the scattered field has a reversal (relative to the pump wave) spatial part and reproduces its temporal structure:

$$\varepsilon_s(t, r) = T(t)P^*(r). \quad (2)$$

The case of "unfactorized" pumping consisting of  $N$  beams uncorrelated with time is considered in Ref. 6. In the case of an interferometer with wavefront-reversing mirrors the above cases are obtained only for: a) zero path difference between the two beams ("factorized" pumping); b) a path difference exceeding the correlation length  $\Delta l \gg 1/\Delta\nu_1$  ("unfactorized" pumping). In order to analyze the experimental situation we need to know the solution of the problem of the scattering of two spatially inhomogeneous light beams with an arbitrary time correlation.

We shall represent a laser wave in the form of a set of plane waves:

$$\varepsilon_l(t, r) = \sum_{m,n} A_{m,n} \exp[i(\omega_l + m\Omega)t - ik_n r]. \quad (3)$$

Here,  $\omega_l$  is the average frequency of the laser radiation;  $\Omega$  is the separation between the neighboring spectral lines satisfying the condition  $\Omega > \Delta\nu_{\text{SpBS}}$ , where  $\Delta\nu_{\text{SpBS}}$  is the width of the spontaneous scattering lines;  $m = 0, \pm 1, \dots, M$  whereas  $n = 0, 1, \dots, N$ . Then in the case of the amplitudes  $a_{m,q}$  of the scattered-field waves of the type

$$\varepsilon_s(t, r) = \sum_{m,q} a_{m,q} \exp[i(\omega_s + m\Omega)t + ik_q r], \quad (4)$$

assuming that the scattering process has reached a steady state and the number of spatial modes is  $N \gg 1$ , we obtain the following system of equations<sup>4</sup>

$$\frac{da_{m,q}}{dz} = \frac{g}{2} \left[ \sum_{\alpha,n} A_{m,q} A_{\alpha,n}^* a_{\alpha,q} + \sum_{\beta,p} A_{\beta,p}^* A_{m,p} a_{\beta,p} \right]. \quad (5)$$

In the case of two beams converging at an angle which is greater than their divergence, the amplitudes  $A_{mn}$  can be represented as follows:

$$\left. \begin{aligned} A_{mn} &= T_m P_n \text{ for } n < N/2 \text{ - first beam,} \\ A_{mn} &= T_m^* P_n \text{ for } n > N/2 \text{ - second beam.} \end{aligned} \right\} \quad (6)$$

We shall continue the analysis under the assumption of equality of the average intensities of both beams

$$\sum_{m,n < N/2} |A_{mn}|^2 = \sum_{m,n > N/2} |A_{mn}|^2 = I \quad (7)$$

and an arbitrary correlation in time:

$$K = \sum_m T_m^* T_m. \quad (8)$$

Normalization of the spatial amplitudes of the waves to unity

$$\sum_{n < N/2} |P_n|^2 = \sum_{n > N/2} |P_n|^2 = 1 \quad (9)$$

and introduction of new variables

$$\left. \begin{aligned} S &= \sum_{\beta,q < N/2} T_\beta^* P_q a_{\beta,q}, & S_1 &= \sum_{\beta,p > N/2} T_\beta^* P_\beta a_{\beta,p}, \\ S' &= \sum_{\beta,p > N/2} T_\beta P_\beta a_{\beta,p}, & S_1' &= \sum_{\beta,q < N/2} T_\beta^* P_\beta a_{\beta,q}, \end{aligned} \right\} \quad (10)$$

allows us to derive from Eqs. (5) and (6), allowing for Eqs. (7)-(10), the following system

$$\left. \begin{aligned} \frac{dS}{dz} &= \frac{g}{2} (2IS + KS_1' + KS'), & \frac{dS_1}{dz} &= \frac{g}{2} (K^* S' + K^* S_1' + 2IS_1), \\ \frac{dS'}{dz} &= \frac{g}{2} (IS' + 2KS_1 + IS_1'), & \frac{dS_1'}{dz} &= \frac{g}{2} (2K^* S + IS_1' + IS'). \end{aligned} \right\} \quad (11)$$

The solutions of the characteristic equation for the increments are

$$\Gamma_1 = g(I + |K|), \quad \Gamma_2 = g(I - |K|), \quad \Gamma_3 = gI, \quad \Gamma_4 = 0 \quad (12)$$

and they correspond to the scattered field configuration with the spatial part reversed  $a_{m,q} \propto P_q^*$  (see Fig. 2).

In the case of the solutions which are not correlated with the spatial structure of the pump wave, it follows directly from Eq. (5)

$$\Gamma_1 = \frac{1}{2} g(I + |K|), \quad \Gamma_2 = \frac{1}{2} g(I - |K|), \quad \Gamma_3 = gI, \quad \Gamma_4 = 0. \quad (13)$$

The solution with a maximum increment corresponds to the case when stimulated emission evolves from spontaneous noise. For example, the maximum increment  $\Gamma_{\text{max}} = g(I + |K|)$  obtained from Eqs. (5) and (11) is

$$\left. \begin{aligned} a_{m,q} &\propto CP_q^* (T_m + |K| T_m^*/K) \exp[g(I + |K|)z], & q < N/2, \\ a_{m,q} &\propto CP_q^* (T_m^* + K T_m/|K|) \exp[g(I + |K|)z], & q > N/2. \end{aligned} \right\} \quad (14)$$

We can see that the temporal structure of the reflected waves is a superposition of the time dependence of both pump beams. Here, it should be pointed out that similar imposition of the temporal behavior of a "foreign" pump wave on the deflected wave is discussed by us also in Ref. 5 for the case of nonthreshold reflection of a weak prolonged signal in the field of a short high-power pulse.

If we know the temporal structure of the reflected waves given by Eq. (14), we can easily calculate the

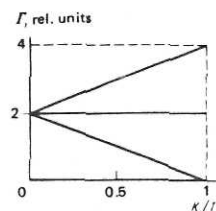


FIG. 2. Dependence of the gain increments of the scattered waves with a field configuration reversed relative to the pump wave on the correlation between the pump beams.

consideration of the reflected waves which interfere at the semitransparent beam-splitting mirror (Fig. 3). I.e., we can plot the visibility curve of the interference pattern:

$$K = \frac{1}{1 + \frac{[K'(\Delta l)]^2}{[K(\Delta l)]^2} + I}. \quad (15)$$

A characteristic feature of this curve is the fact that, in order to find an interferometer with conventional parameters, the interference pattern is not completely visible at large path differences  $2\Delta l$  and the visibility curve reaches a constant level  $V(\infty) = 0.25$ . It should also be noted that when the path difference  $\Delta l$  is increased, there should be a reduction in the efficiency of reflection from a Brillouin mirror, because it follows from Eq. (12) that the scattering increment is  $\Gamma_{\max} = \omega(\Delta l)/\omega_0$  and we recall that  $K \rightarrow 0$  in the limit  $\Delta l \rightarrow \infty$ . It should be stressed that in the theoretical model employed the hypersonic vibrations of the active medium are regarded as monochromatic. This assumption is fully justified because the characteristic time for the change in the phase associated with the nonmonochromaticity of these hypersonic vibrations is  $\tau \sim \Gamma/2\Delta\nu_{\text{SpBS}}$  and for the active medium used in our experiments, which is considerably greater than the duration of the laser pulses.

### 3. EXPERIMENTAL RESULTS AND DISCUSSION

The block diagram of the apparatus used in an experimental study of an interferometer with wavefront-matching is shown in Fig. 3. Multimode laser radiation of wavelength  $\lambda = 633 \mu\text{m}$  was applied through a Fabry-Perot etalon rhomb 2 to a semitransparent mirror 3 with a reflection coefficient  $R = 50\%$ . The radiation transmitted by the mirror 3 was directed to a phase-distorting plate 5. The radiation reflected from a totally reflecting mirror 4 was also directed to the same plate. Movement of the position of the totally reflecting mirror 4 made it possible to vary the path traveled by the beams from the phase-distorting plate 5. An image of a plane of this phase plate illuminated by both beams was projected by a lens onto the end of a lightguide with an active substance 6 placed in such a way as to satisfy the conditions of Eq. (6). The active substance was carbon disulfide and the lightguide was a glass tube 50 cm long with an internal diameter 3 mm. Calorimeters were used to measure the radiation energy flux in the direction opposite to the pump

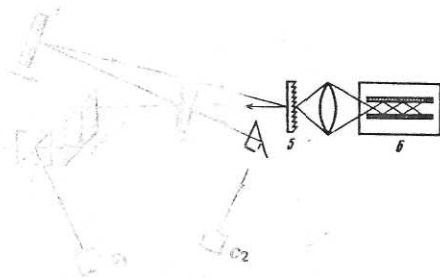


FIG. 3. Block diagram of the apparatus: 1) Glan-Thompson prism; 2) Fabry-Perot rhomb; 3) semitransparent mirror; 4) totally reflecting mirror; 5) phase-distorting plate; 6) lightguide with an active substance.

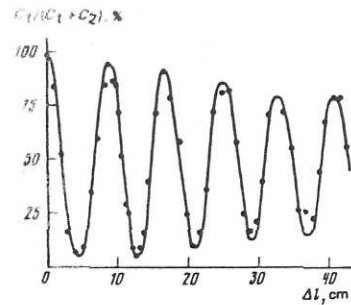


FIG. 4. Interference pattern obtained as a result of variation of the path difference between two pump beams.

( $C_1$ ) and the energy at the exit from the interferometer ( $C_2$ ). The width of the pump line was monitored using a Fabry-Perot etalon with a gap of 3 cm: this width remained constant during our experiments and it amounted to  $\Delta\nu_1 = 0.033 \text{ cm}^{-1} \gg \Delta\nu_{\text{SpBS}} = 4 \times 10^{-3} \text{ cm}^{-1}$  for carbon disulfide (width of the SpBS line was measured by the method of Ref. 5).

Figure 4 shows the experimentally determined dependence of the normalized output energy on the path difference between the two light beams. The characteristic period of this interference pattern was 8 cm. Hence, it was easy to find the Brillouin frequency shift:  $\Delta l \Delta k = 2\pi$ ,  $\Delta l \Delta\nu_B = 1$ , and  $\Delta\nu_B = 0.125 \text{ cm}^{-1}$ . A recalculation of the results obtained at the ruby laser frequency<sup>7</sup> gave  $\Delta\nu_B = 0.116 \text{ cm}^{-1}$ . This difference indicated a considerable dispersion of the velocity of hypersound in carbon disulfide. The results of Fig. 4 also indicated that an increase in the path difference  $\Delta l$  resulted in damping of the interference pattern and a reduction in its visibility.

The values of the visibility of the interference pattern are plotted in Fig. 5. This figure includes also a theoretical curve derived using Eq. (15) in the preceding section on the assumption that the correlation function is Gaussian when the spectral width is  $0.033 \text{ cm}^{-1}$ . We can see that the theoretical curve describes quite satisfactorily the experimental situation.

The theoretical and experimental dependences of the efficiency of reflection on the difference between the beam paths are given in Fig. 6. The experimental points were obtained for fixed values of the intensity of each of the pump beams  $I$  (the threshold intensity for one beam was  $0.9I$ ) and the theoretical curve was plotted assuming that the pump pulse had a triangular envelope and, moreover, that the pump pulse had a triangular envelope and, moreover, that the threshold pump intensity

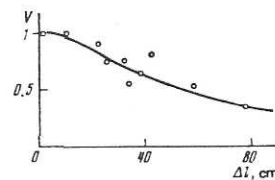


FIG. 5. Visibility  $V$  of an interference pattern for  $\Delta\nu = 0.033 \text{ cm}^{-1}$ : experimental results are represented by points (O) and the theoretical dependence is plotted on the basis of Eq. (15).

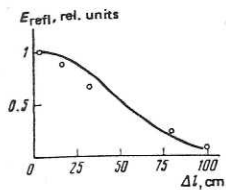


FIG. 6. Dependence of the reflected energy on the path difference between the two pump beams; the experimental results are represented by points (O) and the continuous curve is theoretical.

was governed by the gain increment amounting to  $\Gamma = g(I + |K|) = 10$  [see Eq. (12)]. The assumptions on the nature of the correlation function were the same as in plotting of the theoretical curve in Fig. 5. The good agreement between the experimental and theoretical results in Fig. 6 is additional evidence of the correctness of the adopted theoretical model.

An interferometer system with wavefront-reversing mirrors can also be used to determine an important characteristic of such mirrors, which is the reversal parameter representing the fraction of the energy of the reflected wave in the component relative to the pump wave. The presence in the reflected signal of radiation uncorrelated with the pump wave means that 100% modulation of the interference pattern is not obtained even when the path difference is  $\Delta l \ll 1/\Delta\nu_1$  (see Fig. 4 for  $\Delta l = 0$ ) since the waves uncorrelated with the pump radiation arrive at the semitransparent mirror 3 (Fig. 3) with an arbitrary phase structure. These conclusions were checked for zero path difference between the two beams by measuring the ratio of the calorimeter readings  $C_1/(C_1 + C_2)$  for different phase-distorting plates. The depth of modulation varied from 97% for a plate which increased the divergence of a single-mode helium-neon laser beam from  $5 \times 10^{-4}$  to  $10^{-2}$  rad, to 75% in the absence of a plate of this kind. Hence, in the former case the reversal parameter was 94%, whereas in the latter case it was 50%. The apertures of the beams which could be recorded by these calorimeters were  $10^{-2}$  rad. The precision of this determination of the reversal parameter was considerably greater than the precision of the conventional calorimetric measurements.

#### 4. CONCLUSIONS

We have thus proposed and investigated theoretically and experimentally a two-beam interferometer with

wavefront-reversing StBS mirrors. An important advantage of this interferometer over conventional instruments was its insensitivity to the quality of the optical components of the system and to the spatial structure of the exciting (pump) radiation, as well as the magnification of the interference pattern scale by a factor  $\Delta k_B/k$ . Therefore, an interferometer of this kind could be used in accurate determination of the frequency shift resulting from the Brillouin scattering and in investigations of the structure of laser lines. Moreover, a two-beam interferometer system could be used to carry out direct measurements of the quality of the wavefront-reversal process, which is an important task in the optimization of the parameters of wavefront-reversing mirrors and in verifying the theory of wavefront reversal in StBS.

A system similar to that described above can also be used in practice as a device for effective coupling of radiation out of a system of laser amplifiers because it can act also as an element for decoupling from the reverse pulse. This can be done simply by selecting the difference between the paths of the two beams  $\Delta l = 1/2\Delta k$  (Fig. 1). It is clear that it is also necessary to equalize with sufficient precision the optical paths of the signals in different channels when constructing multichannel laser wavefront-reversing systems in order to ensure that they are in phase at the exit from the system.

- <sup>1</sup>N. G. Basov, V. F. Efimkov, I. G. Zubarev, A. V. Kotov, A. G. Mironov, S. I. Mikhailov, and M. G. Smirnov, *Kvantovaya Elektron. (Moscow)* 6, 765 (1979) [*Sov. J. Quantum Electron.* 9, 455 (1979)].
- <sup>2</sup>Yu. E. D'yakov, *Pis'ma Zh. Eksp. Teor. Fiz.* 10, 545 (1969) [*JETP Lett.* 10, 347 (1969)].
- <sup>3</sup>N. G. Basov, I. G. Zubarev, A. G. Mironov, S. I. Mikhailov, and A. Yu. Okulov, *Pis'ma Zh. Eksp. Teor. Fiz.* 31, 685 (1980) [*JETP Lett.* 31, 645 (1980)].
- <sup>4</sup>L. M. Bel'dyugin, M. G. Galushkin, and E. M. Zemskov, *Kvantovaya Elektron. (Moscow)* 6, 587 (1979) [*Sov. J. Quantum Electron.* 9, 348 (1979)].
- <sup>5</sup>V. F. Efimkov, I. G. Zubarev, A. V. Kotov, A. B. Mironov, S. I. Mikhailov, G. A. Pamanik, M. G. Smirnov, and A. A. Shilov, *Zh. Eksp. Teor. Fiz.* 77, 526 (1979) [*Sov. Phys. JETP* 50, 267 (1979)].
- <sup>6</sup>V. I. Bespalov, V. G. Manishin, and G. A. Pasmanik, *Zh. Eksp. Teor. Fiz.* 77, 1756 (1979) [*Sov. Phys. JETP* 50, 879 (1979)].
- <sup>7</sup>V. S. Starunov and I. L. Fabelinskiĭ, *Usp. Fiz. Nauk* 98, 441 (1969) [*Sov. Phys. Usp.* 12, 463 (1970)].

Translated by A. Tybulewicz